Properties of a Soluble Domain of Subunit C of a Bacterial Nitric Oxide Reductase[†,‡]

Arthur Oubrie,*[,§,||] Sabine Gemeinhardt,[§] Sarah Field,[||] Sophie Marritt,[||] Andrew J. Thomson,[||] Matti Saraste,[§] and David J. Richardson[||]

Structural and Computational Biology Program, European Molecular Biology Laboratory, Meyerhofstrasse 1, D-69117 Heidelberg, Germany, and Centre for Metalloprotein Spectroscopy and Biology, School of Biological Sciences, University of East Anglia, Norwich, NR4 7TJ, United Kingdom

Received May 16, 2002; Revised Manuscript Received July 4, 2002

ABSTRACT: Bacterial nitric oxide reductases are integral membrane proteins that catalyze the reduction of two molecules of nitric oxide to nitrous oxide and water. They are diverged members of the superfamily of heme/copper oxidases. The enzyme from *Paracoccus denitrificans* (NorBC) contains two subunits; NorB comprises the membrane-integrated active site, which harbors a heme iron/non-heme iron dinuclear center. NorC is a membrane-anchored *c*-type cytochrome and presumably the site of electron uptake. A DNA construct encoding the water-soluble domain of NorC ($NorC^{sol}$) was coexpressed with the cytochrome *c* maturation genes in *Escherichia coli*. Using redox potentiometry, electronic absorption, circular dichroism (CD), magnetic CD (MCD), nuclear magnetic resonance, and electron paramagnetic resonance (EPR) spectroscopy the following observations were made: (i) $NorC^{sol}$ was folded into a α-helical structure. (ii) The low-spin heme iron was coordinated by histidine and methionine in both redox states. (iii) The midpoint redox potential of the $NorC^{sol}$ heme was 183 mV, much lower than the corresponding value of 275 mV in the NorBC complex. This points to an increased solvent exposure of the $NorC^{sol}$ heme compared to in the native NorBC complex and shows that the electronic properties of NorC are modulated by NorB in the complex. (iv) The EPR and MCD spectra of $NorC^{sol}$ were considered alongside the spectra of NorBC, which has helped to resolve the contribution that different redox centers make in the holo-enzyme complex.

Bacterial nitric oxide reductases (NORs)[1] are membrane-bound protein complexes that reduce two molecules of nitric oxide (NO) to nitrous oxide and water with concomitant consumption of two electrons and two protons (*1*−*3*). They have a crucial function in denitrification, i.e., the conversion of nitrate to di-nitrogen through a respiratory process in which NO_x compounds are used as terminal electron acceptors. Some NORs may confer resistance to pathogenic bacteria against the toxic NO that is released by macrophages as part of the host defense mechanism. On the basis of amino acid sequence, subunit composition, and the nature of the physiological electron donor, three different types of bacterial NOR can be recognized, which may be exemplified by the enzymes from *Pseudomonas stutzeri* (*4*−*6*) and/or *Paracoccus denitrificans* (*7*−*10*), *Ralstonia eutropha* (*11*, *12*), and *Bacillus azotoformans* (*13*).

The catalytic subunits of all types of bacterial NOR are related and belong to the superfamily of heme/copper oxidases, which includes the mitochondrial cytochrome *c* oxidase (*14*, *15*). The secondary structures, cofactors, and their ligands are very similar, but NORs contain non-heme iron rather than copper in the active site (*10*). The relation between NO reductases and cytochrome oxidases is further illustrated by the discovery that NORs from *Paracoccus* species can reduce di-oxygen (*16*, *17*) and that some oxidases are able to, albeit slowly, reduce NO (*18*). The similarity of the catalytic subunits has led to the hypothesis that NORs and oxidases share a common ancestor (*14*, *19*).

The NOR from *P. denitrificans* is normally purified as a heterodimeric cytochrome *bc* complex (NorBC) (*7*, *9*, *10*). NorC is a membrane-anchored cytochrome *c* that binds heme *c* with a single Cys-Xxx-Xxx-Cys-His heme-binding motif (*7*, *8*). NorB comprises 12 transmembrane α-helices and binds 1 low-spin heme *b*, 1 high-spin heme *b*, and 1 non-heme iron (*10*). The latter two iron sites constitute the dinuclear center, which is the site of NO reduction. The paramagnetic iron atoms are strongly antiferromagnetically coupled (*9*, *10*, *20*) and in close proximity (within 3.5 Å) (*21*).

The mechanism of NO reduction has been studied by analysis of the redox properties of the redox centers (*22*),

[†] Supported by a grant from the European Union Program Biotechnology (Project SENORA BIO4-CT98-0507), BBSRC Grant 83/C10160 to D.J.R. and A.J.T., and long-term EMBO Fellowship ALTF57-2000 to A.O.

[‡] This paper is dedicated to the memory of Matti Saraste.

* To whom correspondence should be addressed at the School of Biological Sciences, University of East Anglia, Norwich NR4 7TJ, United Kingdom. E-mail: a.oubrie@uea.ac.uk; Phone: +44-1603-593796; Fax: +44-1603-592250.

[§] European Molecular Biology Laboratory.

[||] University of East Anglia.

[1] Abbreviations: *ccm*, cytochrome *c* maturation; CD, circular dichroism; *E. coli*, *Escherichia coli*; E_m, midpoint redox potential; EPR, electron-spin paramagnetic resonance; MCD, magnetic circular dichroism; NMR, nuclear magnetic resonance; NO, nitric oxide; NORs, NO reductases; NorB, NOR subunit B; NorBC, NOR consisting of B and C subunits; NorC, NOR subunit C; $NorC^{sol}$, soluble domain of NorC; *P. denitrificans*, *Paracoccus denitrificans*.

10.1021/bi026140y CCC: $22.00
Published on Web 08/02/2002

by mutagenesis of key residues in the active site (*23*), and by the reaction of carbon monoxide with the reduced dinuclear center (*24*, *25*). In contrast, the process of electron uptake by NorBC is only poorly understood. NorBC has been suggested to take electrons from soluble donors such as cytochromes and cupredoxins (*3*, *26*, *27*), but so far a role as electron donor has only been shown directly for cytochrome c_{550} (*16*). Electron uptake could be mediated by NorC (*3*, *8*, *27*), but no experimental data have so far been reported.

The interaction between NorC and NorB was studied by the cloning and expression in *Escherichia coli* of a part of the *norC* gene that encodes a water-soluble domain of NorC ($NorC^{sol}$). Assembly of this domain was facilitated by coexpression of the host-specific cytochrome *c* maturation (*ccm*) genes (*28*). $NorC^{sol}$ was properly folded into a predominantly α-helical structure. The heme iron displays a low midpoint redox potential (E_m), suggestive of a partially solvent-exposed heme. This feature hints at a modulation of the redox properties of NorC by NorB in the complex and thus at a functional interaction between these two subunits. In addition, the data of $NorC^{sol}$ have facilitated resolving the electron paramagnetic resonance (EPR) and magnetic circular dichroism (MCD) spectra of the native NorBC complex.

EXPERIMENTAL PROCEDURES

Cloning of NorC. All DNA manipulations were performed using standard protocols (*29*). *E. coli* strain DH5α was used in cloning procedures. Primers were designed on the basis of the reported sequence of NorC (*8*) and obtained from Sigma-Ark. The oligonucleotides NorC1_forward (5′-CATGCCATGGTCGTCGAGGGCAAGCATAT-3′) and NorC1_reverse (5′-CGGGATCCTCAGCCCGCGTCGTTCGGTGG-3′) were used as forward and reverse primers, respectively. NorC1_forward contained an *Nco*I restriction site and encoded the peptide VVEGKHI, while NorC1_reverse contained a *Bam*HI restriction site and was complementary to the 3′-end of *NorC*. Using these primers, a 303 bp fragment coding for NorC was amplified from plasmid pPnir3E (kindly provided by Rob van Spanning, University of Amsterdam) (*8*). The PCR product was inserted into vector pET-22b(+) (Novagen), which carries an ampicillin-resistance cassette, to yield plasmid pNORC1. This plasmid was sequenced on both strands by Sequence Laboratories Göttingen to check for correct incorporation of the insert.

Bacterial Strains and Growth Conditions. *E. coli* strain BL21(DE3) (Novagen) was used for heterologous expression of NorC of *P. denitrificans*. Cells were transformed sequentially with plasmids pNORC1 and pEC86, which confers chloramphenicol resistance and carries all eight *ccm* genes of *E. coli* (*28*). Cells were grown aerobically at 37 °C on plates with Luria−Bertani (LB) medium, containing 50 μg/mL ampicillin and 34 μg/mL chloramphenicol. The resultant colonies were used to inoculate 4 L of LB medium, supplemented with the appropriate antibiotics, 1% glycerol, and 0.3 mg/mL $MgSO_4$. Cells were grown aerobically for 18 h at 27 °C to reach an optical density of 3.6 at 600 nm. They were collected by centrifugation at 4500 rpm for 20 min at 4 °C and resuspended in fresh medium containing 1 mM IPTG for induction. After 3.5 h of aerobic growth at 25 °C, cells were harvested by centrifugation at 5000 rpm for 30 min at 4 °C. Freezing of the cells was avoided to prevent lysis.

Purification of NorC. For preparation of periplasmic fractions (*30*), 39 g of wet cells freshly harvested from 4 L of culture was resuspended in 200 mM Tris/HCl, pH 8.0, and a ratio of 10 mL of buffer per gram of wet cells was used. The suspension was diluted 2-fold with a buffer containing 1 M sucrose, 1 mM EDTA, 1 mM Pefabloc SC, 200 mM Tris/HCl, pH 8 (*31*). Lysozyme was added to a final concentration of 60 μg/mL. To perform a mild osmotic shock, the suspension was diluted 2-fold with H_2O followed by gentle stirring on ice for 30 min. To stabilize the spheroplasts, 20 mM $MgCl_2$ was added, and the suspension was centrifuged at 7000 rpm for 30 min at 4 °C. The red supernatant was applied to a DEAE Sepharose Fast Flow anion exchange column (5 × 10 cm, Pharmacia) preequilibrated with 20 mM NaCl, 0.5 mM EDTA, 20 mM Tris/HCl, pH 8 (buffer A). Unbound protein was washed off with 1 column volume of buffer A, and the NorC fragment was eluted in 5 column volumes with a linear gradient of 20−500 mM NaCl (in buffer A). Fractions enriched in heme *c* were pooled and diluted 3-fold with 0.5 mM EDTA, 20 mM Tris/HCl, pH 8. They were applied to a 53 mL Q-Sepharose fast flow column (Pharmacia), which was preequilibrated with 50 mM NaCl, 0.5 mM EDTA, 20 mM Tris/HCl, pH 8 (buffer B). After being washed with 1 column volume of buffer B, bound protein was eluted in 11.5 column volumes with a linear gradient of 50−800 mM NaCl (in buffer B). NorC-containing fractions were collected and concentrated to 1 mL in Centriprep Centrifugal Filter Devices with a cutoff of 10 kDa. Protein batches of 200 μL were applied to a Sephacryl 100 gel filtration column (1 × 30 cm, Pharmacia) that was preequilibrated with 100 mM NaCl, 0.5 mM EDTA, 20 mM Tris/HCl, pH 8. Fractions containing pure NorC were concentrated to 9 mg/mL. Protein aliquots were flash-frozen in liquid nitrogen and stored at −80 °C.

Protein and Heme Determinations. Protein expression and the purity of protein samples were assessed by using polyacrylamide gel electrophoresis (*29*). The presence of *c*-type hemes on gels was detected by incubation with tetramethylbenzidine and staining with hydrogen peroxide (*32*). Protein concentrations were estimated using the Bradford assay (BioRad) and by recording redox difference optical spectra at 551 nm. A protein mass spectrum was recorded on a Quadrupole Time-of-Flight Electrospray Tandem Mass Spectrometer (Micromass) at the Proteomics Visitor Facility of the European Molecular Biology Laboratory (Heidelberg, Germany).

Spectroscopic Methods. One-dimensional proton nuclear magnetic resonance (NMR) spectra were acquired at 295 K on a Bruker DRX500 spectrometer. A WATERGATE scheme was used for suppression of the water signal (*33*). The sample of 0.2 mM NorC in the redox state as purified was in 20 mM phosphate, pH 6.9. Circular dichroism (CD) spectra of a 10 μM sample in 20 mM phosphate, pH 7.0, were recorded on a Jasco J-710 spectropolarimeter using a cell with a 1 mm optical path length. Usually, 20 scans were acquired in the range 190−250 nm at a temperature of 283 K by taking points every 0.2 nm, with 100 nm min^{-1} scan rate, an integration time of 1 s, and a 1 nm bandwidth. The secondary structure content of α-helices was estimated according to the method of Greenfield and Fasman (*34*). EPR spectra of ferricyanide-oxidized NorC were collected at 10 K using 2 mW microwave power on an ER-200D X-band

spectrometer (Bruker Spectrospin) interfaced to an ESP1600 computer and fitted with a liquid-helium flow cryostat (ESR-9; Oxford Instruments). Ultraviolet−visible region spectra were recorded using an Aminco SLM DW2000 spectrophotometer. UV−visible MCD spectra were recorded at room temperature on a Jasco J-710 spectropolarimeter with a magnetic field of 6 T applied using an Oxford Instruments SM-1 superconducting magnet. All spectra were exported as ASCII files and replotted in Origin 6.1 (Microcal).

Redox Potentiometry. Mediated redox titrations with NorC^{sol} and the *Paracoccus* NorBC were carried out under identical, low ionic strength conditions, i.e., at 298 K in 20 mM Bis-Tris propane, pH 7.0. Dithionite was used as reductant and ferricyanide as oxidant. Redox mediators were phenazine methosulfate, phenazine ethosulfate, tetramethyl-*p*-phenyldiamine, menadione, 2,6-dimethylbenzaquinone, benzyl viologen, and anthraquinone-2,6-disulfonate (at a final concentration of 14 μM). A saturated quinhydrone solution, having an E_m of +295 mV, was used for calibration of the instrumentation. All potentials were measured with respect to the normal hydrogen electrode. Redox titrations were fitted using a customized program in Table-Curve 2D (Jandel Scientific).

RESULTS

Expression and Purification of NorC^{sol}. A *norC* DNA fragment encoding a water-soluble domain of NorC (NorC^{sol}) was cloned from plasmid pPnir3E, which encodes all six genes of the *nor* operon of *P. denitrificans* (*8*), and ligated into pET-22b(+) to yield pNORC1. The construct contains the *pelB* signal sequence for targeting to the periplasm, a single methionine as a result of the cloning strategy, and the 101 amino acid *NorC* fragment starting with the sequence VVEGKH. Subsequent sequencing on both strands confirmed the amino acid sequence of the fragment to be as published previously. Heterologous production of NorC^{sol} in the periplasmic compartment of *E. coli* was achieved by coexpression of the *ccm* genes. Successful targeting to the periplasm and incorporation of heme *c* were indicated by the appearance of red color in the bacterial cells and periplasmic fractions. Redox difference electronic absorption spectra of periplasmic fractions exhibited a clear peak at 551 nm, which is indicative for the presence of heme *c* (not shown).

NorC^{sol} was purified from 4 L cultures of *E. coli* (pNORC1) A typical preparation yielded 18 mg of pure protein. The apo-enzyme, without heme *c*, has a calculated molecular mass of 11 647 Da. The holo-enzyme with heme covalently bound should thus have a molecular mass of ca. 12.3 kDa. This is in excellent agreement with the molecular mass as determined by SDS-gel electrophoresis and electrospray mass spectrometry. The mass spectrum (not shown) shows three series of peaks. The dominant series of peaks has a molecular mass of 12 262 Da and is due to holo-enzyme and its sodium adducts. A second series with the most intense peak at 11 645 Da represents an apo-enzyme form, i.e., without heme. A third peak at 11 953.4 Da represents a small percentage (3−4%) of a contaminating species.

NMR and CD Spectroscopy of NorC^{sol}. The proton NMR spectrum of as-purified, ferrous NorC^{sol} exhibits a multitude of sharp peaks dispersed over a broad frequency range (−3 to 11 ppm) (Figure 1). At least 13 proton resonances can be recognized at high field (below 0 ppm), of which 3 are below −2 ppm and characteristic of heme with His-Met iron ligation. Four features can be recognized in the far-UV CD spectrum between 190 and 250 nm (Figure 2). These are a strong positive band at 195 nm and a strong negative band at 208 nm, as well as weak negative bands at about 215 and 233 nm. The signals at 208 and 215 nm are diagnostic for the presence of α-helical structure. Using the method of Greenfield and Fasman (*34*), the helical content was estimated to be 37% for the soluble domain. The band at 233 nm is attributed to a contribution from random coil (*35*).

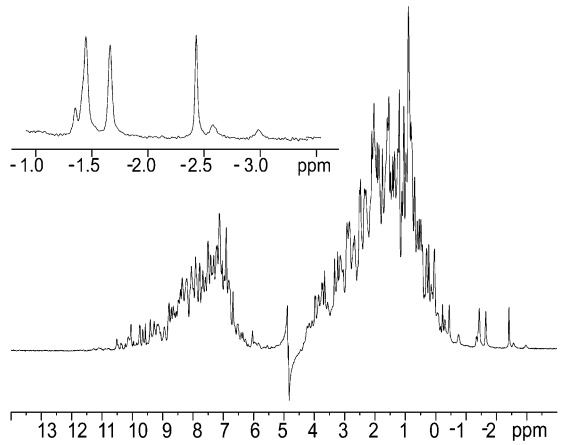

FIGURE 1: One-dimensional proton NMR spectrum of *P. denitrificans* NorC^{sol}. The spectrum was acquired at 295 K on a 500 MHz Bruker spectrometer. The sample of 0.2 mM NorC in the redox state as-purified was in 20 mM phosphate, pH 6.9. The inset shows the low-field part of the spectrum. Diagnostic for methionine as heme iron ligand are signals at −2.4, −2.6, and −3.0 ppm.

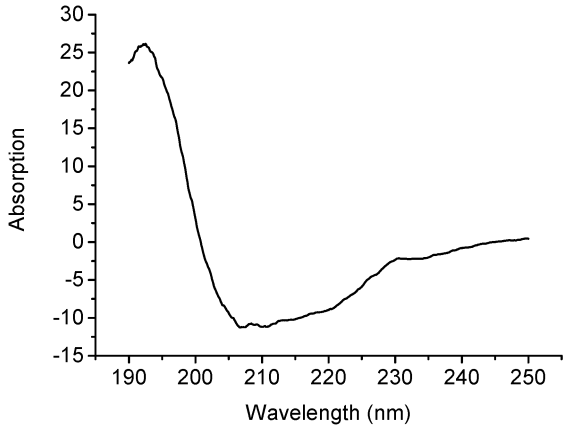

FIGURE 2: CD spectrum of the far-UV region of NorC^{sol} from *P. denitrificans*. The 10 μM NorC sample was in 20 mM phosphate, pH 7.0. The spectrum was recorded at 283 K on a Jasco J-710 spectropolarimeter using a cell with a 1 mm optical path length. 20 scans were acquired by taking points every 0.2 nm, with 100 nm min^{-1} scan rate, an integration time of 1 s, and a 1 nm bandwidth. Bands at 195, 208, 215, and 233 nm can be identified. On the basis of the 208 nm band, the helical content was calculated to be 37% for NorC^{sol}.

Spectropotentiometric Analysis of NorC^{sol}. The electronic absorption spectrum of ferricyanide-oxidized NorC^{sol} exhibits a broad peak with a maximum at 525 nm and a shoulder at 552 nm, which are assigned to the β- and α-bands of the low-spin heme *c*, respectively (Figure 3A). The same bands give rise to sharp peaks with maxima at 522 and 551 nm in the dithionite-reduced spectrum (Figure 3A). There are no

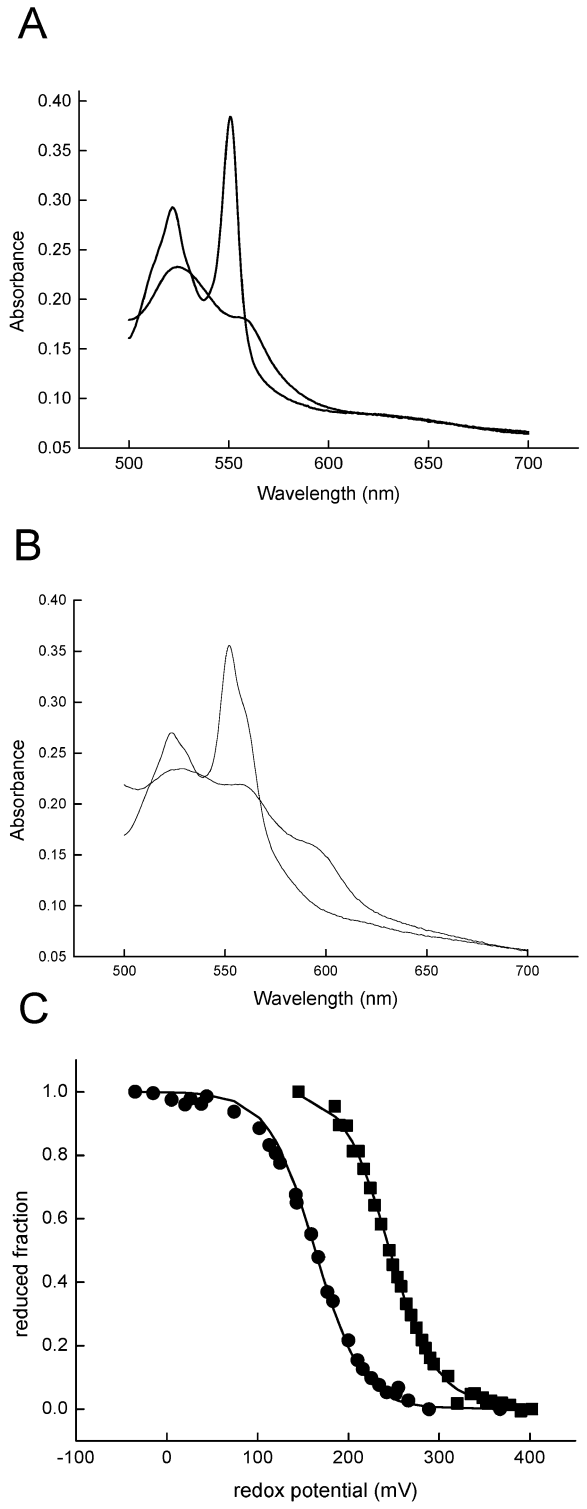

FIGURE 3: Electronic absorption spectra and redox titers of *P. denitrificans* NorC^{sol} and native NorBC. (A) Absorption spectra of reduced and oxidized NorC^{sol}. (B) Absorption spectra of reduced and oxidized NorBC. (C) Redox titer for NorC^{sol} (circles) and NorBC (squares). Mediated redox titrations were carried out at 298 K in 20 mM Bis-Tris propane, pH 7.0. The data are fitted to single-component $n = 1$ Nernstian curves. Reductive and oxidative titrations were identical. The midpoint redox potentials of the *c*-type heme in NorC and NorBC were +183 and +275 mV, respectively. The reduced fraction was calculated from the $\Delta A_{550-700nm}$ at each potential by dividing by the $\Delta A_{550-700nm}$ of the fully reduced *minus* fully oxidized sample.

signals for other types of heme. The absorbance shoulders at 560 nm in reduced NorBC and at 595 nm in oxidized

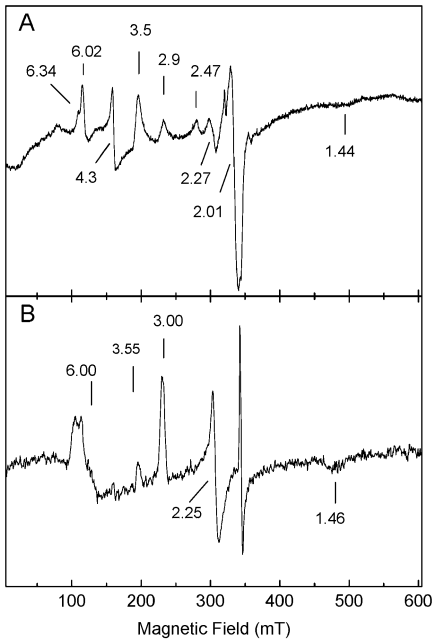

FIGURE 4: X-band EPR spectra of NorC^{sol} (A) and NorBC (B) from *P. denitrificans*. Both samples were oxidized with ferricyanide. The spectrum was recorded at 10 K using 2 mW microwave power. The *g*-values of features discussed in the text are indicated.

NorBC (Figure 3B) are absent in NorC^{sol}, confirming that these arise from the two NorB hemes in the native NorBC complex. Visible region electronic absorption spectra of NorC^{sol} and NorBC were recorded between 500 and 700 nm at a range of electrochemical potentials. Starting from ferricyanide-oxidized protein, an increase in intensity at 551 nm was observed after every addition of dithionite when going from ca. +400 mV to −50 mV (reductive curve). The absorption differences at 551−700 nm over this potential range were plotted as a function of potential. Reductive and oxidative titrations were identical, and points from both experiments were included in Figure 3C. An E_m of +183 mV was derived by fitting a single component $n = 1$ Nernstian curve to the data (Figure 3C). By comparison, the corresponding E_m of the low-spin heme *c* of NorBC, under identical buffer conditions, was +275 mV, some 90 mV higher than NorC^{sol}.

MCD and EPR Spectroscopy. The low-temperature EPR spectrum of ferricyanide-oxidized NorC (Figure 4A) shows a signal at $g = 3.5$, which is assigned to the g_z component of the spectrum of a low-spin ferric heme *c*. This signal has an asymmetric shape, the left slope being much steeper than the right one. The high *g* value and the asymmetric shape of the signal together indicate that it is the g_z component of a rhombic trio in which the other two *g* values are broad, making them difficult to detect (*36*). Such a signal is often called the 'high g_{max}' signal and is also clearly resolved in the NorBC spectrum (Figure 4B). There has been some debate over which heme this arises from in NorBC (*6*, *14*, *17*), but this analysis confirms that it is due to the NorC subunit. Three features at $g = 2.9$, 2.27, and 1.44 are assigned to a rhombic trio of low-spin ferric *c*-type heme. This feature is clearly much weaker than that observed in NorBC, from which it can be concluded that this feature arises from the low-spin heme *b* in the native heterodimeric enzyme. In terms of spin concentration, the ratio of Fe(III) contributing to these

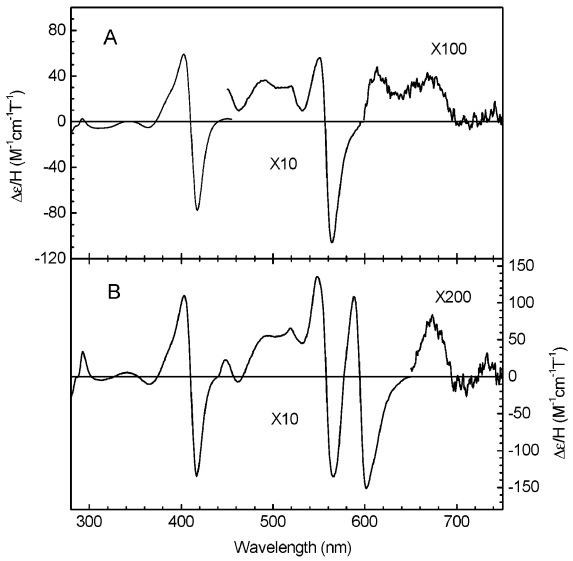

FIGURE 5: UV−visible region RT-MCD spectrum of NorC^{sol} (A) and NorBC (B) from *P. denitrificans*. Both samples were oxidized with ferricyanide. [NorC] was 180 μM in 20 mM Bis-Tris propane, 50 mM NaCl, pH 7.0, 0.05% dodecyl maltoside. [NorBC] was 175 μM in 20 mM Tris-HCl, pH 7.6, 0.02% dodecyl maltoside. $\Delta\epsilon/H$ values are quoted with respect to protein concentration as calculated from the heme absorption spectrum.

two heme signals in NorC^{sol} is about 0.9:0.1 for the 'high g_{max}' 'rhombic trio'. Signals at $g = 4.3$ and $g = 2.0$ are due to adventitious high-spin non-heme iron and copper, respectively. Small amounts of high-spin heme iron and of hydroxide-bound high-spin heme iron give rise to the features near $g = 6$ and $g = 2.47$, respectively. The MCD spectrum of NorC^{sol} (Figure 5A) is characteristic of low-spin ferric heme. Porphyrin-based $\pi-\pi^*$ transitions contribute to the Soret derivative, centered at 410 nm, and the α, β region at 530−560 nm. However, the weak absorption features between 640 and 740 nm are characteristic of S→Fe(III) charge-transfer bands arising from the Met-S−Fe heme ligand. This confirms that in the ferric state the NorC^{sol} has histidine−methionine heme iron ligation. The weak feature in the NorC^{sol} spectrum at around 620 nm probably arises from small amounts of bis-hydroxide-bound high-spin heme that was also revealed by EPR spectroscopy. A derivative feature at 595 nm in the NorBC spectrum (Figure 5B) is absent from NorC^{sol}.

DISCUSSION

In the present study, we have cloned and expressed a soluble, functional domain comprising the C-terminal 101 amino acids of subunit C of the *P. denitrificans* NOR. Successful production of holo-enzyme was achieved by coexpression of the *ccm* cluster of *E. coli*. Previous expression studies of *c*-type cytochromes in *E. coli* have shown that significant quantities of mature enzyme can only be produced by constitutive coexpression of that cluster (*28, 37*). NorC^{sol} was purified in good yield, enabling some important structural and spectroscopic information to be obtained.

The CD spectrum of NorC^{sol} confirmed that it adopted a folded conformation, and the percentage of α-helix was calculated to be 37%. This is in the range of published values for other cytochromes; for example, values of 33, 43, and 50% have been reported for the Class 1 monoheme cytochromes from *P. denitrificans* (*38*), *Hydrogenobacter thermophilus* (*39*), and horse heart (*40*). The feature at 234 nm in the CD spectrum is attributed to a contribution from random coil. The NorC sequence is considerably longer than the approximately 80 residues that are necessary to form the cytochrome *c* core structure, so it may have considerable loop regions.

That NorC^{sol} adopts a folded conformation was also confirmed by the ^{1}H NMR spectrum of the as-purified, ferrous protein, which displayed numerous, sharp and intense peaks dispersed over a broad frequency range. This is as expected for folded protein samples. Denatured NorC^{sol} would have had chemical shifts close to those found for short linear peptides, and the resonances would thus cluster around 0.8−1.1 ppm (methyl groups), 4.1−4.4 ppm (α-protons), and 8−8.5 ppm (amide protons) (*41*). At least 13 proton resonances can be recognized below 0 ppm in the proton NMR spectrum. This is a common feature in NMR spectra of cytochromes *c* and is related to the magnetic properties of the heme iron. A total of 10 and 20 of such signals have been recognized in NMR spectra of oxidized (*42*) and reduced (*43*) forms of a soluble domain of cytochrome c_{552} of *P. denitrificans*. They have been assigned to hydrogen atoms belonging to 6 leucines, 2 valines, 1 glycine, 1 proline, and the heme iron methionine ligand. Structure determinations by X-ray crystallography (*38*) and NMR spectroscopy (*44*) have shown that these residues form the hydrophobic heme-binding pocket and are consequently close to the heme iron. By analogy to the assignment for cytochrome c_{552}, the presence of high-field resonances in the NMR spectrum of NorC^{sol} suggests that several amino acids are in close proximity to the heme iron, and this provides further confirmation of correct protein folding. Resonance assignment to specific hydrogen atoms would provide substantial structural information on the residues involved in heme binding and form an excellent starting point for a three-dimensional structure determination by NMR spectroscopic methods.

Among the 13 low-frequency resonances, 3 are located below −2.0 ppm, well resolved from other signals. These resonances, at −2.4, −2.6, and −3.0 ppm, are diagnostic for the presence of a heme iron methionine ligand. The general pattern of such methionine resonances consists of three weak and one relatively intense peak, where the latter peak is due to the singlet of the three methyl group protons of methionine (*45*). One of the weak signals has not been recognized in the NMR spectrum; it possibly resonates at a somewhat higher frequency (above −1.0 ppm). A similar distribution of the methionine frequencies has been found previously for the heme-coordinating methionine of cytochrome c_{551} from the purple phototrophic bacterium *Ectothiorhodospira halophila* (*46*). From the NMR spectrum, it can thus be concluded that the ferrous heme iron has histidine and methionine as axial ligands.

Two low-spin heme signals are present in the EPR spectrum, one rhombic trio with $g_z = 3.5$ and unknown g_x and g_y as well as a second rhombic trio at $g = 2.9$, 2.3, and 1.4. The former signal is also present in EPR spectra of NorBC complexes as can be seen from the spectrum of the *P. denitrificans* species in Figure 4B (*9, 22*). Assignment of the resonances of this spectrum has so far been ambiguous.

The relevant signals are at $g = 3.5$, 3.0, 2.3, and 1.4. They have been assigned to a high g_{max} value at $g = 3.5$ from a low-spin heme *c* and a rhombic trio at $g = 3.0$, 2.3, and 1.4 from a low-spin heme *b* for preparations from *P. denitrificans* (*22*) and *Pseudomonas stutzeri* (*20*). Alternatively, the same resonances have been attributed to a rhombic trio from heme *c* and a high g_{max} signal from a low-spin heme *b* for NorBC from two *Paracoccus* species (*9, 17*). As NorC^{sol} gives rise to a $g = 3.5$ resonance, we can now conclude that the virtually identical signal in NorBC spectra must also be due to heme *c*. It has been shown for the NorBC preparation (*22*) that the heme that gives rise to the high g_{max} value has histidine and methionine as axial ligands and this most likely holds for NorC^{sol} as well. The first case of a His−Met coordinated heme with a high *g* value was reported in cytochrome c_4 from *Azotobacter vinelandii*, which contains an asymmetric EPR signal at $g = 3.64$ and the other at $g = 3.22$, 2.10, and 1.17. The high g_{max} signal requires that the two axial ligands generate an effective pseudo-four-fold axis; that is, the heme *x* and *y* axes are electronically equivalent. This constrains the orientation of the methionine group to be parallel to that of the histidine plane (*47*).

There are several possible explanations for the presence of the second rhombic trio at $g = 2.9$, 2.3, and 1.4 in the NorC^{sol} spectrum. First of all, this signal could be due to a contamination (of a 12.0 kDa protein) that is seen by mass spectrometry. In this case, a low-spin heme coordinated by two histidines with approximately parallel ligand plane orientations (*36*) or a low-spin heme with histidine and methionine as axial ligands (*45*) account for the signal. However, it is not at all certain that the alleged contaminant is a hemoprotein capable of causing the EPR signal. The expression host *E. coli* hardly produces any cytochromes *c* under aerobic conditions, and we have not resolved a 12.0 kDa band on SDS gels.

If the contaminant does not contain heme, then the rhombic trio at $g = 2.9$, 2.3, and 1.4 should be assigned to a second active site conformer of NorC^{sol}. Given the resonance frequencies, the axial ligands could be either histidine or methionine. Apart from the histidine of the heme *c* binding motif, there is only one other histidine in NorC^{sol}. This residue is not conserved among NorC sequences, and it is located on the N-terminal side of the heme-binding motif, a region of the sequence far away from the heme iron in most cytochrome *c* structures. The second histidine is therefore not likely to serve as an axial ligand for the heme iron. Instead, the rhombic trio would then be assigned to heme *c* with histidine and methionine coordination, so both EPR signals would be due to the same heme *c* with identical axial ligands. To give rise to two signals, one of the ligands must adopt two distinct conformations. The histidine of the heme-binding motif invariantly coordinates the heme iron with its NE2 atom in a fixed orientation (*45*), so the conformational flexibility is most likely due to the methionine. The features at $g = 2.9$, 2.3, and 1.4 have not been observed in any preparation of NorBC. There are two possible explanations for this. The methionine conformation that possibly gives rise to these signals could be absent in NorBC preparations. On the other hand, the signals could be present but unnoticed so far. This is not unlikely as the *g*-values of the rhombic trio of the histidine−methionine coordinated heme *c* (2.9, 2.3, and 1.4) are virtually identical to those of the low-spin heme *b* with bis-histidine ligation (3.0, 2.3, and 1.4) present in NorB. In any case, the peaks representing the alternative methionine conformation are small; the signal at $g = 2.9$, for example, has an intensity of about 9−10% of the same resonance attributed to the low-spin heme *b* in NorBC. This indicates that a relatively small but significant fraction of the methionines would adopt the alternative conformation. It could be speculated that flexibility of the distal ligand may be important for electron transfer from NorC to the low-spine heme *b* in NorB.

The resolution of S→Fe(III) charge-transfer bands in the MCD spectrum of NorC^{sol} served to confirm His-Met heme iron ligation in the ferric state. The quantification of the different MCD signals also proves informative. The peak to trough intensity of the derivative centered at 680 nm is ca. 0.5 M^{-1} cm^{-1} T^{-1} in both NorC^{sol} and NorBC, suggesting that in NorBC this absorption band is predominantly contributed by NorC heme. The peak to trough intensity of the Soret band for NorC^{sol} is ca. 125 M^{-1} cm^{-1} T^{-1}, a value consistent with one low-spin ferric heme. This compares to ca. 250 M^{-1} cm^{-1} T^{-1} in NorBC where two low-spin hemes are contributing to the Soret absorbance, the NorC heme *c* and NorB heme *b*. Interpretation of the region of the MCD between 530 and 630 nm in ferric NorBC has proved difficult. The NorC^{sol} MCD spectrum may help to clarify this region. The peak to trough intensity of the '560 nm' derivative of NorC^{sol} is ca. 12 M^{-1} cm^{-1} T^{-1}. This compares to ca. 25 M^{-1} cm^{-1} T^{-1} for NorBC and suggests that in the latter two low-spin hemes are contributing to this absorption envelope. These would likely be the low-spin hemes *c* and *b* as suggested for *Ps. stutzeri* (*17*). However, it has previously been questioned whether both hemes do contribute to this absorption in *P. denitrificans NorBC*. The present comparison with NorC^{sol} would suggest that they do and raise the possibility that the derivative centered at 595 nm in NorBC arises from the μ-oxo-bridged high-spin heme b_3, even though it is 2−3 times larger than normally expected for high-spin heme.

The E_m values of the heme cofactors have been determined both in NorC^{sol} and in the NorBC complex. The values of the *c*-type heme are +183 and +275 mV, respectively. As the experiments were carried out under identical experimental conditions and spectroscopy indicates the coordination of the iron and the axial ligand to be identical in both redox states, the dramatic increase of the E_m by about 100 mV in NorBC is likely to be a direct/indirect result of the presence/addition of the NorB subunit. Macromolecular ligands, of which NorB is an example, have previously been shown to have a substantial effect on the E_m (*45*). Matching of the potential does not seem important for electron transfer from NorC to NorB because both E_m values of +183 and +275 mV enable such transfer to the *b*-type heme ($E_m = +345$ mV). Instead, elevation of the potential to +275 mV upon addition of NorB could prepare NorC for acceptance of electrons from the putative physiological electron donors cytochrome c_{550} ($E_m = +265$ mV) and pseudoazurin ($E_m = +230$ mV). E_m modulation of the heme *c* thus seems important for inter-protein rather than intraprotein electron transfer.

Addition of NorB to NorC may affect the E_m of the latter by altering its active site and/or electrostatic properties. An alteration in the active site could in principle be brought about by a ligand switch. However, all spectroscopic data indicate

that the *c*-heme is ligated by histidine and methionine in both redox states of NorC as well as NorBC. As there is no indication that the metal coordination or iron−sulfur bond is affected, these factors are not likely to have contributed to the observed E_m change. Thus, it seems likely that the dramatic influence of NorB on the potential of NorC is due to differential electrostatic interactions with the bulk solvent. More specifically, some charged residues may be exposed to solvent in NorC but buried in the NorBC complex. In addition, the heme may be relatively buried in the NorBC complex but more solvent-exposed in isolated NorC.

The currently determined E_m of 275 mV for the heme *c* in the NorBC complex is significantly lower than the value of 310 mV that was reported previously for this heme (*22*). The 35 mV difference is due to different experimental conditions. The current experiment was carried out at a pH of 7, whereas the previous determination was conducted at pH 7.6 and in the presence of 340 mM NaCl. Changes in pH and/or ionic strength are known to affect the E_m on the basis of similar underlying chemical principles (*45*). An acidic protein such as NorC (with a p*I* of 4.8) is negatively charged at pH 7.0−7.6, and the reduced state is more negatively charged than the oxidized state. The reduced state is more likely to bind protons and is more stabilized at lower pH. Thus, by lowering the pH from 7.7 to 7, the E_m should *increase*. Similarly, the reduced state is stabilized more than the oxidized state by the presence of counterions, leading to an increase of the redox potential as a function of the ionic strength. By reducing the ionic strength by 340 mM NaCl, the E_m should *decrease*. Thus, the variations of pH and ionic strength have had counteracting effects, and apparently the change of ionic strength has a stronger influence (by 35 mV) than that of pH.

In conclusion, a soluble domain of NorC was cloned, expressed, purified, and characterized by a variety of spectroscopic and potentiometric techniques. It was shown that this domain had significant α-helical content and that the heme iron was coordinated by histidine and methionine ligands in the oxidized as well as the reduced enzyme forms. The midpoint redox potential of the *c*-type heme of NorC in isolation was about 100 mV lower than in NorBC, which provides evidence that the soluble domain of subunit C makes a direct, functional interaction with the catalytic subunit B. Finally, the careful spectroscopic characterization made it possible to assign with certainty the EPR and MCD spectra of the holo-enzyme complex.

ACKNOWLEDGMENT

We are grateful to Rob van Spanning, Bernd Ludwig, and Linda Thöny-Meyer for kind gifts of plasmids pNir3E and pEC86, and to Arie Geerlof for preparation of plasmid pET-22b(+) and advice in the cloning stages of this project. We thank Silke Wiesner and Miles Cheesman for assistance in collecting the NMR and EPR spectra, respectively, Janneke Hendriks for carefully reading the manuscript, and Nicholas Watmough for stimulating discussions.

REFERENCES

1. Zumft, W. G. (1997) *Microbiol. Mol. Biol. Rev. 61*, 533−616.
2. Watmough, N. J., Butland, G., Cheesman, M. R., Moir, J. W., Richardson, D. J., and Spiro, S. (1999) *Biochim. Biophys. Acta 1411*, 456−474.
3. Hendriks, J., Oubrie, A., Castresana, J., Urbani, A., Gemeinhardt, S., and Saraste, M. (2000) *Biochim. Biophys. Acta 1459*, 266−273.
4. Heiss, B., Frunzke, K., and Zumft, W. G. (1989) *J. Bacteriol. 171*, 3288−3297.
5. Braun, C., and Zumft, W. G. (1991) *J. Biol. Chem. 266*, 22785−22788.
6. Braun, C., and Zumft, W. G. (1992) *J. Bacteriol. 174*, 2394−2397.
7. Carr, G. J., and Ferguson, S. J. (1990) *Biochem. J. 269*, 423−429.
8. de Boer, A. P., van der Oost, J., Reijnders, W. N., Westerhoff, H. V., Stouthamer, A. H., and van Spanning, R. J. (1996) *Eur. J. Biochem. 242*, 592−600.
9. Girsch, P., and de Vries, S. (1997) *Biochim. Biophys. Acta 1318*, 202−216.
10. Hendriks, J., Warne, A., Gohlke, U., Haltia, T., Ludovici, C., Lubben, M., and Saraste, M. (1998) *Biochemistry 37*, 13102−13109.
11. Cramm, R., Siddiqui, R. A., and Friedrich, B. (1997) *J. Bacteriol. 179*, 6769−6777.
12. Cramm, R., Pohlmann, A., and Friedrich, B. (1999) *FEBS Lett. 460*, 6−10.
13. Suharti, Strampraad, M. J., Schroder, I., and de Vries, S. (2001) *Biochemistry 40*, 2632−2639.
14. Saraste, M., and Castresana, J. (1994) *FEBS Lett. 341*, 1−4.
15. van der Oost, J., de Boer, A. P., de Gier, J. W., Zumft, W. G., Stouthamer, A. H., and van Spanning, R. J. (1994) *FEMS Microbiol. Lett. 121*, 1−9.
16. Fujiwara, T., and Fukumori, Y. (1996) *J. Bacteriol. 178*, 1866−1871.
17. Sakurai, N., and Sakurai, T. (1997) *Biochemistry 36*, 13809−13815.
18. Giuffre, A., Stubauer, G., Sarti, P., Brunori, M., Zumft, W. G., Buse, G., and Soulimane, T. (1999) *Proc. Natl. Acad. Sci. U.S.A. 96*, 14718−14723.
19. Castresana, J., and Saraste, M. (1995) *Trends Biochem. Sci. 20*, 443−448.
20. Cheesman, M. R., Zumft, W. G., and Thomson, A. J. (1998) *Biochemistry 37*, 3994−4000.
21. Moënne-Loccoz, P., Richter, O.-M. H., Huang, H.-W., Wasser, I. M., Ghiladi, R. A., Karlin, K. D., and de Vries, S. (2000) *J. Am. Chem. Soc. 122*, 9344−9345.
22. Grönberg, K. L., Roldan, M. D., Prior, L., Butland, G., Cheesman, M. R., Richardson, D. J., Spiro, S., Thomson, A. J., and Watmough, N. J. (1999) *Biochemistry 38*, 13780−13786.
23. Butland, G., Spiro, S., Watmough, N. J., and Richardson, D. J. (2001) *J. Bacteriol. 183*, 189−199.
24. Moënne-Loccoz, P., and de Vries, S. (1998) *J. Am. Chem. Soc. 120*, 5147−5152.
25. Hendriks, J. H., Prior, L., Baker, A. R., Thomson, A. J., Saraste, M., and Watmough, N. J. (2001) *Biochemistry 40*, 13361−13369.
26. Berks, B. C., Ferguson, S. J., Moir, J. W., and Richardson, D. J. (1995) *Biochim. Biophys. Acta 1232*, 97−173.
27. Hendriks, J., Gohlke, U., and Saraste, M. (1998) *J. Bioenerg. Biomembr. 30*, 15−24.
28. Arslan, E., Schulz, H., Zufferey, R., Kunzler, P., and Thony-Meyer, L. (1998) *Biochem. Biophys. Res. Commun. 251*, 744−747.
29. Sambrook, J., Fritsch, F. E., and Maniatis, T. (1989) *Molecular cloning: A laboratory manual*, 2nd ed., Cold Spring Harbor Laboratory, Cold Spring Harbor, NY.
30. Witholt, B., Boekhout, M., Brock, M., Kingma, J., van Heerikhuizen, H., and de Leij, L. (1976) *Anal. Biochem. 74*, 160−170.
31. Dean, C. R., and Ward, O. P. (1992) *Biotechnol. Tech. 6*, 133−138.
32. Thomas, P. E., Ryan, D., and Levin, W. (1976) *Anal. Biochem. 75*, 168−176.
33. Piotto, M., Saudek, V., and Sklenar, V. (1992) *J. Biomol. NMR 2*, 661−665.
34. Greenfield, N., and Fasman, G. D. (1969) *Biochemistry 8*, 4108−4116.
35. Rodger, A., and Norden, B. (1997) *Circular dichroism and linear dichroism*, Oxford University Press, Oxford, U.K.

36. Walker, F. A., Huynh, B. H., Scheidt, W. R., and Osvath, S. R. (1986) *J. Am. Chem. Soc. 108*, 5288−5297.
37. Reincke, B., Thony-Meyer, L., Dannehl, C., Odenwald, A., Aidim, M., Witt, H., Ruterjans, H., and Ludwig, B. (1999) *Biochim. Biophys. Acta 1411*, 114−120.
38. Harrenga, A., Reincke, B., Ruterjans, H., Ludwig, B., and Michel, H. (2000) *J. Mol. Biol. 295*, 667−678.
39. Wain, R., Pertinhez, T. A., Tomlinson, E. J., Hong, L., Dobson, C. M., Ferguson, S. J., and Smith, L. J. (2001) *J. Biol. Chem. 276*, 45813−45817.
40. Akiyama, S., Takahashi, S., Ishimori, K., and Morishima, I. (2000) *Nat. Struct. Biol. 7*, 514−520.
41. Cavanagh, J., Fairbrother, W. J., Palmer, A. G., III, and Skelton, N. J. (1996) *Protein NMR spectroscopy: Principles and practice*, Academic Press, Inc., San Diego.
42. Lücke, C., Reincke, B., Löhr, F., Pristovšek, P., Ludwig, B., and Rüterjans, H. (2000) *J. Biomol. NMR 18*, 365−366.
43. Pristovšek, P., Lücke, C., Reincke, B., Löhr, F., Ludwig, B., and Rüterjans, H. (2000) *J. Biomol. NMR 16*, 353−354.
44. Pristovšek, P., Lücke, C., Reincke, B., Ludwig, B., and Rüterjans, H. (2000) *Eur. J. Biochem. 267*, 4205−4212.
45. Moore, G. R., and Pettigrew, G. W. (1990) *Cytochromes c: Evolutionary, structural and physicochemical aspects*, Springer-Verlag, Berlin and Heidelberg.
46. Bersch, B., Brutscher, B., Meyer, T. E., and Marion, D. (1995) *Eur. J. Biochem. 227*, 249−260.
47. Gadsby, P. M., Hartshorn, R. T., Moura, J. J., Sinclair-Day, J. D., Sykes, A. G., and Thomson, A. J. (1989) *Biochim. Biophys. Acta 994*, 37−46.

BI026140Y